

## Effect of Copper Species in a Photocatalytic Synthesis of Methanol from Carbon Dioxide over Copper-doped Titania Catalysts

<sup>1</sup>Slamet, <sup>1</sup>Hosna W. Nasution, <sup>1</sup>Ezza Purnama, <sup>2</sup>Kapti Riyani and <sup>2</sup>Jarnuzi Gunlazuardi

<sup>1</sup>Department of Chemical Engineering, University of Indonesia, Depok 16424, Indonesia

<sup>2</sup>Department of Chemistry, University of Indonesia, Depok 16424, Indonesia

**Abstract:** Synthesis of methanol from CO<sub>2</sub> by a photocatalytic reduction process over copper-doped TiO<sub>2</sub> has been investigated. It has been reported in the literature that copper species could enhance methanol production in a photocatalytic reduction of CO<sub>2</sub>. However, which species of copper (e.g. Cu<sup>0</sup>, Cu<sup>I</sup>, or Cu<sup>II</sup>) and how do the copper species play a role still unclear. In this paper we will report and discuss our finding that each copper species play a different role. By using modified-impregnation method in preparing copper/TiO<sub>2</sub> it was revealed that CuO is the copper species, which resulting much better enhancement in methanol production than the others. The activation energy (E<sub>a</sub>) for TiO<sub>2</sub> Degussa-P25 and 3%CuO/TiO<sub>2</sub> is ca. 26 and 12 kJ/mol, respectively. The lower E<sub>a</sub> of 3%CuO/TiO<sub>2</sub> may suggest a catalytic role of copper species that increase the methanol production. Furthermore, an *in situ* FTIR study revealed appearance of formate and methoxy intermediates on the CuO/TiO<sub>2</sub> surface, while none if the undoped TiO<sub>2</sub> catalyst was employed. This may indicate a catalytic nature of copper species as an active site to give methanol. Enhancement of product yield was also observed indicates that the copper species act as an electron trapper and prohibit electron-hole recombination.

**Key words:** Photocatalytic reduction • Titanium dioxide • Copper species • CO<sub>2</sub> • Methanol

### INTRODUCTION

The continuously increasing CO<sub>2</sub> level into the atmosphere is one of the most serious problems with regard to the greenhouse effect. Photocatalytic reduction of CO<sub>2</sub> become in the future an alternative solution not only for environmental problems caused by CO<sub>2</sub> emission, but also for finding ways to maintain hydrocarbon resources which now on are being dominated by fuel and natural gas. Methanol as one of the main product of CO<sub>2</sub> photoreduction can be transformed into other useful chemicals and used as fuel-like renewable energy [1]. Much research has been reported that CO<sub>2</sub>, in the present of water, can be photocatalytically converted to methane, methanol, or other hydrocarbons over TiO<sub>2</sub> or copper doped TiO<sub>2</sub> [1-5], CoPc loaded TiO<sub>2</sub> [6] and mixed oxide-based photocatalyst [7,8]. It is likely that the efficiency and selectivity of the product depend on the type of catalyst. The most crucial problem is a low quantum yield in the photocatalysis process due to electron and positive hole recombination, hence produce only limited reduction species on catalyst surface.

In order to solve low quantum yield and selectivity problems many researchers attempted to modify TiO<sub>2</sub> by doping it with metal impurities. Many transition metal ion dopants have been demonstrated to enhance the rate of photocatalytic oxidation or reduction by changing the dynamics of electron-hole recombination and interfacial charge transfer [9]. In CO<sub>2</sub> photoreduction, Yamashita *et al.* [3] reported that addition of copper (II) to the TiO<sub>2</sub> matrix could improve the efficiency and selectivity to produce methanol. It was suggested however that copper in the first oxidation state (Cu<sup>I</sup>) might play a significant role in the formation of methanol [3]. Tseng *et al.* has found that the formation of methanol much more effective on Cu-titania catalysts, that the copper species were predominantly Cu<sub>2</sub>O [1]. Other investigators also noted that addition of copper could improve the photocatalytic activity in CO<sub>2</sub> reduction, without exactly noticing in which species they are present [2,10]. It is therefore important to investigate how and which copper species (Cu<sup>0</sup>, Cu<sup>I</sup>, or Cu<sup>II</sup>) actually has a significant contribution in improving the CO<sub>2</sub> photocatalytic reduction over TiO<sub>2</sub> matrix.

In the present study, we will report and discuss our finding that each copper species play a different role. A modified preparation method has been conducted to synthesize a  $\text{Cu}^0/\text{TiO}_2$ ,  $\text{Cu}^{\text{I}}/\text{TiO}_2$  and  $\text{Cu}^{\text{II}}/\text{TiO}_2$  catalysts. The measurement of these catalysts by means of XRD, UV-vis diffuse reflectance spectroscopy (DRS), SEM/EDAX/Mapping and BET have been carried out to investigate the characteristics of the catalysts. Special attention has been focused on the relationship between the copper species and the photoefficiency of methanol formation. Therefore temperature dependence of the reaction and *in situ* FTIR study were also performed to clarify the kinetic and mechanistic aspects, respectively.

## MATERIALS AND METHODS

### Preparation and Characterization of Catalysts:

Copper/ $\text{TiO}_2$  catalysts were prepared by impregnating  $\text{TiO}_2$  Degussa-P25 with copper nitrate solution to give copper content that varies between 0.5 and 10 wt%. The improved-impregnation method was done by conventional impregnation process that followed by sonication of the impregnated  $\text{TiO}_2$  slurry, stirring of the slurry at 368 K, drying followed by calcination and reduction-oxidation treatment to form  $\text{Cu}^0/\text{TiO}_2$  and  $\text{Cu}^{\text{I}}/\text{TiO}_2$  catalysts. Product of the atmospheric calcination step (773 K, 0.5 h) is predicted to be in the form of  $\text{CuO}/\text{TiO}_2$ . Reduction step under 100 ml/min of 20% $\text{H}_2$ -He mixture at 573 K for 3 hours was completed to make a metallic copper form ( $\text{Cu}^0/\text{TiO}_2$ ). The final step of oxidation was performed under 100 ml/min of  $\text{N}_2\text{O}$  at 353 K for 3 h to get  $\text{Cu}_2\text{O}/\text{TiO}_2$ .

The specific surface area of catalysts was measured by multipoint BET of  $\text{N}_2$  adsorption at 77 K in a Quantachrome Autosorb-6. Prior to BET analysis, the catalysts were degassed at 423 K under vacuum for 10-12 h. The crystalline phase of the catalysts was identified using powder X-ray diffraction (XRD). The XRD patterns were obtained from a PHILIPS PW 1710 using Ni-filtered Cu  $K\alpha$  radiation ( $\lambda=0.154184$  nm) that operated at 40 kV and 30 mA. The  $2\theta$  scanning range was  $23^\circ$ - $63^\circ$  with a step size of  $0.01^\circ$  and a time per step of 1.0 s. The crystallite sizes of the samples were estimated from FWHM (full-width at half-maximum) of XRD by Scherrer equation. A Cary 2415 UV-vis-NIR spectrophotometer equipped with an integrated sphere was used to record the diffuse reflectance spectra (DRS) of the catalysts. The reflectance spectra of the samples were recorded under ambient condition in the wavelength range of 340-700 nm. A SEM 515 PHILIPS scanning electron microscope (SEM)

equipped with EDAX PV9900 PHILIPS energy dispersive X-ray (EDX) and Mapping was conducted at 15 kV and 22 kV to observe the morphology of catalysts, to perform semi-quantitative analysis and to analyze distribution of Cu, respectively.

**Photocatalytic Reaction:** The photocatalytic reduction of  $\text{CO}_2$  under UV light was carried out in a reactor system that schematically illustrated in Fig. 1. A flat top cover of the vessel was made of Pyrex and equipped with a gas bubbler and sampling port. The reactor vessel was irradiated, from top of the reactor, by 6 Toki tubular black light UV lamps (@ 10 W), which have the radiation peak about 365 nm. As measured with Black Ray Ultraviolet Meter Model 1225, the UV lamps had total intensity of  $2450 \mu\text{W}/\text{cm}^2$  in the surface of the catalyst slurry. The reactor was enclosed by an aluminium foil reflector to optimize UV irradiation and to prevent interference from outside light. The reaction temperature was controlled with hot plate magnetic stirrer and fan cooler.

Previous to photoreactions, blank experiments were conducted to ensure that the product formed was due to the photoreduction of  $\text{CO}_2$ . The blank tests consist of the solution illuminated without the catalyst and a reaction in the dark with the catalyst. Reaction suspensions were prepared by using 300 ml of 1 M  $\text{KHCO}_3$  solution and 0.3 g of catalyst powder was added, subsequently followed by sonication for 30 min. Ultra High Purity (UHP) grade  $\text{CO}_2$  is bubbled through the reactor for at least 30 min to purge air and to saturate the suspension. The reactor is tightly closed during the reaction and a magnetic stirrer agitated the catalyst-suspended solution at the bottom to prevent sedimentation of the catalyst. The liquid sample was withdrawn every hour from a reactor column. The catalyst-suspended samples were centrifuged to separate catalyst particles from the liquid samples and then analyzed by a GC-FID of Shimadzu 8-ATC equipped with Porapak-Q column.

The *in situ* IR spectra were measured using an IR quartz reactor cell equipped with ZnSe windows and connected to a conventional vacuum system. The catalysts (27.5 mg) were pressed into a 10 mm diameter disk and then placed in the cell. Prior to photoreactions and IR measurements, the catalysts were heated at 423 K for 2 h and then evacuated at  $2 \times 10^{-2}$  torr. UV irradiation of the catalysts in the presence of  $\text{CO}_2$  (330  $\mu\text{mol}$ ) and gaseous  $\text{H}_2\text{O}$  (1650  $\mu\text{mol}$ ) was carried out using the Toki black light UV lamps at 333 K. The spectra on catalyst surface were periodically recorded using a Genesis series FTIR Spectrometer ATI Mattson. Each spectrum was

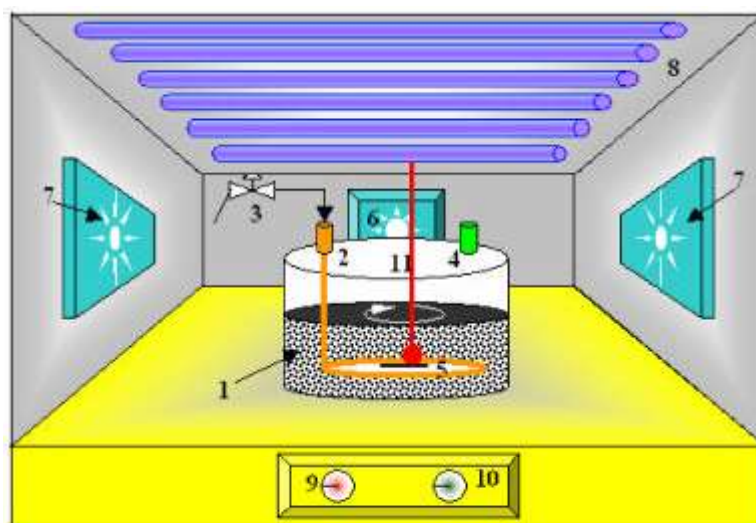


Fig. 1: The scheme of the photocatalytic reaction system

(1 = Stainless steel vessel, 2 = Gas bubbler, 3 = Control valve, 4 = Sampling Port, 5 = Magnetic stirrer bar, 6 = Inlet fan, 7 = Outlet fan, 8 = UV lamps, 9 = Temperature regulator, 10 = Speed regulator, 11 = Thermometer)

recorded by averaging 150 scans at an instrument resolution of  $4\text{ cm}^{-1}$ .

## RESULTS AND DISCUSSION

**Physical Characterization:** As shown in Fig. 2, SEM analysis of the catalysts indicated that addition of Cu on  $\text{TiO}_2$  can affect the surface morphology of the catalyst; however there is no significant effect on the aggregate sizes. The aggregate sizes of the catalysts were relatively uniform, ranging from 0.4 to  $1.0\text{ }\mu\text{m}$ . The EDX/Mapping analysis of Cu on the catalysts demonstrated that Cu uniformly dispersed on  $\text{TiO}_2$  surface and further increase of copper leads to the increase of the peak as well as the dot intensities of Cu (inset of Fig. 2).

Figure 3 displays the XRD spectra of the Degussa P25 and copper/ $\text{TiO}_2$  of various copper loadings. The peaks on  $2\theta = 25.3^\circ$  and  $2\theta = 27.4^\circ$  correspond to the main peak of anatase and rutile, respectively. It can be confirmed that for all copper modified  $\text{TiO}_2$  samples, only the characteristic peaks corresponding to P25 were found (which consisted of 79% anatase and 21% rutile). Small diffraction peaks of CuO appeared near  $2\theta = 35.6^\circ$  and  $2\theta = 38.8^\circ$  only on the high CuO loading samples ( $\geq 3\%$ ) and the peak intensities increase for higher CuO loading. The crystalline size of anatase and rutile were relatively uniform, ranging from 19 to 22 nm and 23 to 31 nm, respectively. Whereas the copper species clusters grew up from 16 to 25 nm with increasing of the loading from 3 to 10 wt%, respectively. No CuO peaks were observed

on the low CuO loading samples is due to either the slight amount of copper loading or very small CuO particle size that results in high dispersion of the dopant species. In addition, the disappearance of the CuO peaks after reduction of the samples (Fig. 3-d') verified that CuO has been successfully reduced to other species.

The dispersion capacity of CuO on  $\text{TiO}_2$  (anatase) should be equal to the number of the surface octahedral vacant sites available in the preferentially exposed (001) plane of anatase, i.e.,  $6.98\text{ Cu}^{2+}\text{ nm}^{-2}$  [11]. When the CuO loading exceeds its dispersion capacity, all the vacant sites have been occupied and then the existence of crystalline CuO can be detected by XRD. Plotted in inset of Fig. 3 is the ratio of the XRD peak intensities of CuO and  $\text{TiO}_2$  vs. the loading amounts of CuO in the samples, from which the dispersion capacity of CuO on  $\text{TiO}_2$  P25 (79% anatase and 21% rutile) is determined to be 2.2 wt.% ( $4.16\text{ Cu}^{2+}\text{ nm}^{-2}$ ). Whereas Xu *et al.* [11] have investigated that the dispersion capacity of CuO on  $\text{TiO}_2$  (pure anatase) is about  $6.74\text{ Cu}^{2+}\text{ nm}^{-2}$ . The discrepancy of this dispersion capacity may be caused by the different  $\text{TiO}_2$  crystalline used as precursor as well as the higher of thermal treatment in this work.

The DRS patterns of  $\text{TiO}_2$  P25 and all CuO-loaded samples are shown in Fig. 4. The figure shows that the spectra of copper-titania catalysts are different from unmodified  $\text{TiO}_2$  P25. Surface modification of  $\text{TiO}_2$  with copper significantly affects the absorption properties of the catalysts. The absorption spectra were obtained by analyzing the reflectance measurement with

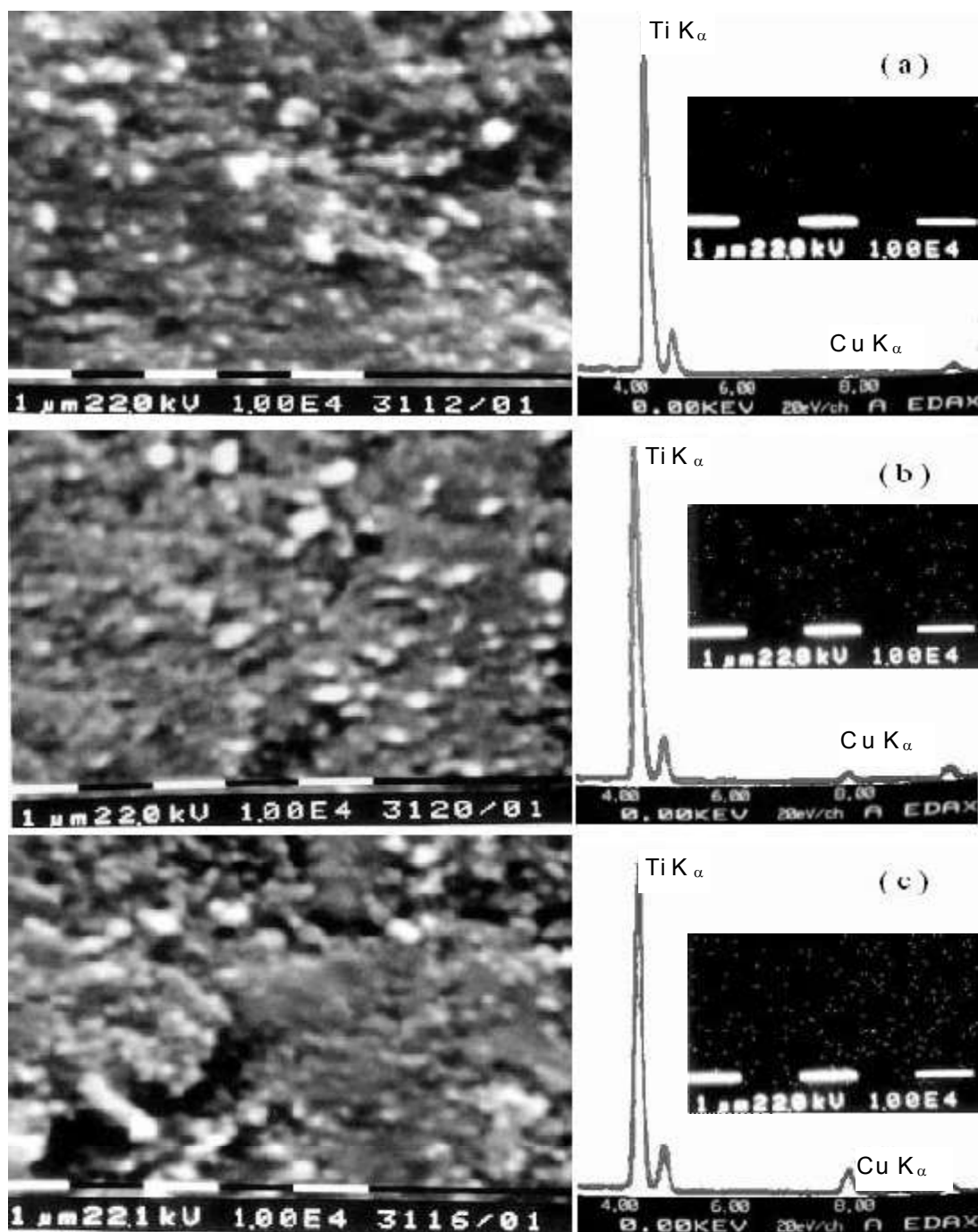


Fig. 2: SEM (left) and EDX (right) images of the catalysts. Inset: mapping images of Cu (a = 1%CuO/TiO<sub>2</sub>; b = 5%CuO/TiO<sub>2</sub>; c = 10%CuO/TiO<sub>2</sub>)

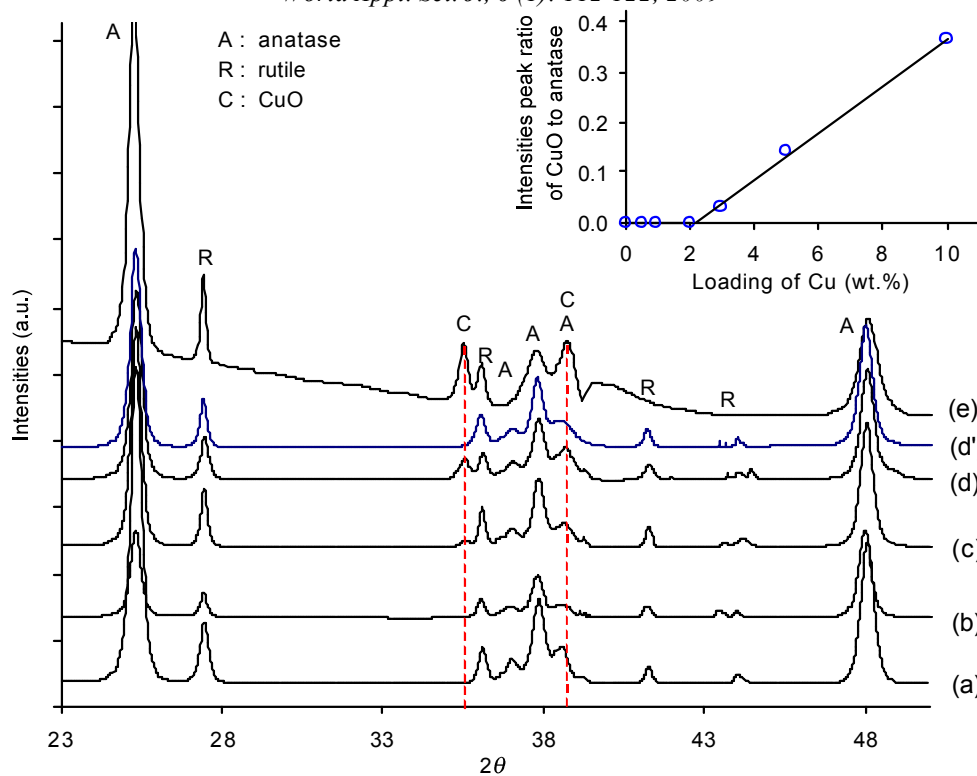


Fig. 3: XRD spectra of prepared catalysts: (a)  $\text{TiO}_2$ -P25, (b) 1%CuO/ $\text{TiO}_2$ , (c) 3%CuO/ $\text{TiO}_2$ , (d) 5%CuO/ $\text{TiO}_2$ , (d') reduced-5%CuO/ $\text{TiO}_2$ , (e) 10%CuO/ $\text{TiO}_2$ .  
Inset: plot of quantitative analysis of the XRD data

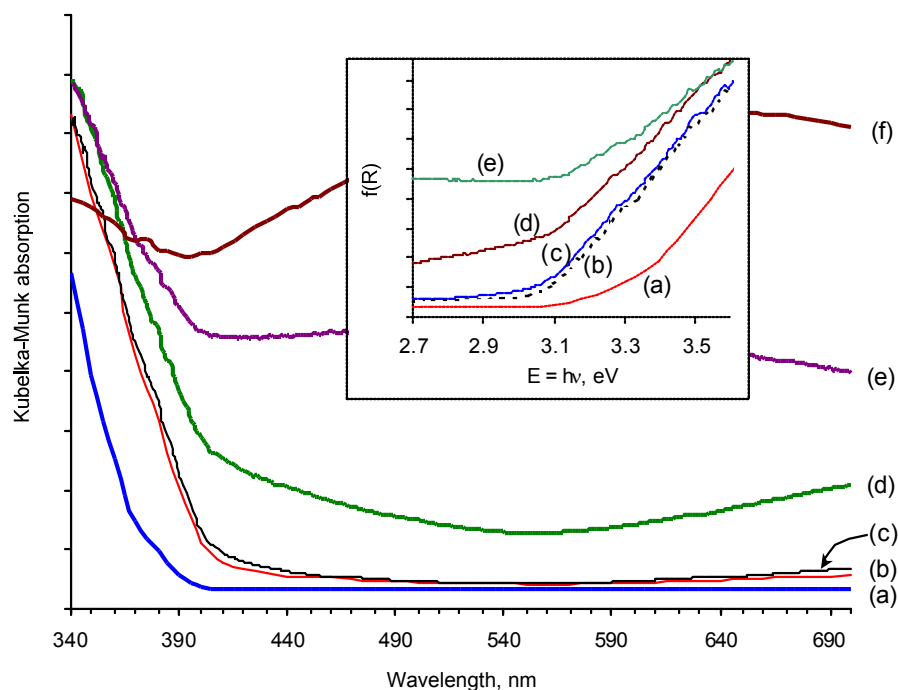


Fig. 4: DRS patterns of copper-titania catalysts: (a)  $\text{TiO}_2$  (P25), (b) 0.5%CuO/ $\text{TiO}_2$ , (c) 1%CuO/ $\text{TiO}_2$ , (d) 3%CuO/ $\text{TiO}_2$ , (e) 5%CuO/ $\text{TiO}_2$ , (f) 10%CuO/ $\text{TiO}_2$ .  
Inset: plot of bandgap estimation

Kubelka-Munk emission function [9]. It is noticeable that the absorbance of the copper loaded samples increases with increasing Cu content. The absorption edge of  $\text{TiO}_2$  shifts toward the visible region upon the addition of copper and the baseline in the visible light region is clearly raised.

The bandgap can be estimated by extrapolating the rising segment of the UV spectrum to the abscissa at zero absorption [12]. As shown in inset of Fig. 4, the bandgap of the modified catalysts decreased with increasing of copper loaded. Remarkably, the bandgap is governed by the crystalline structure and the defects in the  $\text{TiO}_2$  network. Sanchez *et al.* [12] suggested that small bandgaps were caused by the stoichiometric deficiency of Ti/O ratio.

A specific surface area of unmodified titania catalyst was  $54 \text{ m}^2/\text{g}$ , whereas the surface area of copper-loaded titania samples were relatively uniform, ranging from  $45$  to  $50 \text{ m}^2/\text{g}$ . It can be inferred that copper loading on the  $\text{TiO}_2$  surface did not significantly change the surface area of the catalysts. A small decrease in some catalysts was caused by thermal treatment during the preparation. The surface area values are only somewhat decreased with increase of copper loading. Apparently, the slight change in surface area does not contribute to the reactivity of the catalyst.

**Photocatalytic Activity:** Figure 5 presents the rate of methanol formation on illumination time for various catalysts. Methanol yield was used to evaluate the performance of the catalysts, as it was the major product. Ethanol, propanol, acetone and other hydrocarbons (included oxalate, formate and  $\text{CH}_2\text{O}$ ) might have been generated, but in small quantities which is too low to be detected. Blank experiments, in the absence of  $\text{TiO}_2$  as well as in the dark reaction, showed that there was no organic product found for long periods of  $\text{CO}_2$  photoreduction. Various yields of methanol were obtained in a period depending on the type of catalysts. The maximum methanol yield was achieved by 3%CuO/ $\text{TiO}_2$  representing that this catalyst had the highest reactivity among all the prepared catalysts.

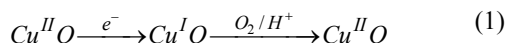
Figure 6 plots the effect of copper loading on methanol yields, indicating that the methanol yields increased with Cu loading, but then decreased when the Cu loading exceeded 3 wt%. Obviously, more Cu loading can increase methanol yield owing to the amount of active sites. Copper can serve as an electron trapper and prohibits the electron-hole recombination, significantly increasing photoefficiency [1]. However, catalysts with

more than 3 wt% Cu loading cannot further increase the methanol yield due to its shading effects which are much higher, consequently reducing the photo exciting capacity of  $\text{TiO}_2$ . Therefore it is estimated, under the experimental conditions of this work, that an optimum amount of copper loading is approximately 3 wt%.

As shown in DRS patterns (Fig. 4), the absorption spectra of low copper-loaded catalysts ( $\leq 3 \text{ wt}\%$  Cu) were not far different from  $\text{TiO}_2$  P25 pattern and only shifted to the visible region. It can be supposed, as reported by Anpo *et al.* [13], that in this case implanted metal ions do not work as electron-hole recombination centers but only work to modify the electronic properties of the catalyst. The band gap values of the copper-loaded catalysts, as revealed in Fig. 4, were smaller than  $\text{TiO}_2$ ; consequently the photon energy needed to excite electron would not be too high and furthermore it can increase the photoactivity of  $\text{TiO}_2$ . The dispersion capacity of 2.2 wt% Cu, as evaluated by XRD analysis, indicated that the increasing of CuO above 2.2 wt% might increase the shading effects. However below 3 wt% loading, we found that its shading effects could still be covered by its high ability to trap electrons.

Figure 6 also demonstrates that CuO is the most active dopant comparing with the other species. The formation of methanol was found to be much more effective on  $\text{Cu}^{2+}$  loaded  $\text{TiO}_2$  catalyst. One of the considerations in selecting copper oxide as dopant is based on their potential redox position as well as the potential redox value, which is represents their ability to attract electrons. From a thermodynamic perspective, trapping electron by metal ions ( $\text{Cu}^+$  or  $\text{Cu}^{2+}$ ) within the semiconductor photocatalyst is feasible due to the reduction potential of the metal ions is more positive than the conduction band edge of  $\text{TiO}_2$  ( $\approx -0.2 \text{ V}$ ) [9]. The positive potential redox value of  $\text{Cu}^+$  is higher than that of  $\text{Cu}^{2+}$  (0.52 vs. 0.34 V); therefore  $\text{Cu}_2\text{O}$  dopant should effectively act as an electron trapper to prohibit electron-hole recombination. However, owing to the relatively strong interaction between  $\text{TiO}_2$  and the dopant particle implanted in the vacant sites of  $\text{TiO}_2$ , the dopant with more positive potential redox exceedingly catches electron from conduction band edge. As a result the dopant-trapped electrons are more difficult to be transformed to the adsorbed species on catalyst surface. The smaller activity of  $\text{Cu}^I$  and  $\text{Cu}^0$  species is not associated with lower selectivity by methanol formation due to undetectable of other products in all species of copper-doped Titania catalysts.

On the contrary,  $\text{Cu}^{2+}$  with the lower potential redox is a more promising dopant species. Due to the reduction of  $\text{Cu}^{2+}$  is thermodynamically feasible and a  $\text{Cu}^{2+}$  ion has an unfilled 3d shell, it is valid to assume that electrons can be trapped by  $\text{Cu}^{\text{II}}\text{O}$  on the surface of  $\text{TiO}_2$  [9]. Figure 7 and equation (1) illustrate the redox cycle of  $\text{Cu}^{2+}/\text{Cu}^+$  that maybe played by  $\text{CuO}$  dopant on the  $\text{TiO}_2$  matrix. Part of the photo-excited electrons on the conduction band ( $e_{\text{CB}}^-$ ) will be trapped by  $\text{Cu}^{2+}$ , consequently the species of  $\text{Cu}^{2+}$  can be reduced to  $\text{Cu}^+$  species. Trapped electrons could be consumed via the reduction of  $\text{H}^+$  and/or  $\text{O}_2$  that present in the system forming radicals of  $\bullet\text{H}$  and/or  $\bullet\text{O}_2^-$ , respectively. Consequently, the  $\text{Cu}^+$  species could be re-oxidized again to  $\text{Cu}^{2+}$  species. As a result of this sequential cycle, the electron-hole recombination rate could be effectively reduced. In addition,  $\text{Cu}^+$  species could act as a main adsorption site of  $\text{CO}_2$  for methanol synthesis [14]. Furthermore, the fixation of  $\text{CO}_2$  via  $\bullet\text{H}$  radicals can lead to methanol formation [7].



To study the kinetic aspect of the  $\text{CO}_2$  photoreduction, the experiment was repeated at different temperatures in the range of 316-373 K. Inset of Fig. 6 shows a typical Arrhenius plot for Degussa P25 and 3% $\text{CuO}/\text{TiO}_2$  catalysts. A mean value for apparent activation energy ( $E_a$ ) of ca. +26 and +12 kJ/mol was calculated for Degussa P25 and 3% $\text{CuO}/\text{TiO}_2$ , respectively. Determination of the  $E_a$  value is quite accurate due to the coefficient correlation  $R^2$  is in the range of 0.90-0.93. These positive values of  $E_a$  imply that the desorption of products is the rate limiting step in the photosynthetic formation of methanol [15]. In addition, the lower  $E_a$  of 3% $\text{CuO}/\text{TiO}_2$  catalyst may indicate a catalytic role of copper species as an active site to provide methanol and hence improving the photoefficiency of  $\text{TiO}_2$  photocatalyst. Guan *et al.* [16] reported that in the photocatalytic reduction of  $\text{CO}_2$  under concentrated sunlight,  $\text{CH}_3\text{OH}$  was catalytically formed over the  $\text{Cu}/\text{ZnO}$  catalyst if it combined with  $\text{K}_2\text{Ti}_6\text{O}_{13}$  photocatalyst.

The *in situ* IR experiments were conducted to investigate the mechanism aspects of the catalyst. Figure 8 shows the *in situ* IR spectra of 3% $\text{CuO}/\text{TiO}_2$  catalyst during gas phase  $\text{CO}_2$  photoreduction as a function of time irradiation. The methanol product was identified by growing up of the absorption bands at 1430-1560  $\text{cm}^{-1}$ , which are attributed to  $\delta(\text{CH}_3)$ . The absorption bands at 1360 and 2867  $\text{cm}^{-1}$  also correspond

to lewis bound of  $\text{CH}_3\text{OH}$   $\delta_s(\text{OH})$  and lewis bound of  $\text{CH}_3\text{OH}$   $\delta_s(\text{CH}_3)$ , respectively. The band at 2968  $\text{cm}^{-1}$  corresponds to  $\nu_{\text{as}}(\text{CH}_3)$  [17,18]. Although the bands at 2600-3000  $\text{cm}^{-1}$  are not completely clear caused by close to noise, a formate species adsorbed on Ti are observed at 1544, 2873, 2950  $\text{cm}^{-1}$  and the bands at 2845, 2939, 1373  $\text{cm}^{-1}$  are assigned to formate-Cu species. These formate species adsorbed on Cu and Ti can be regarded as an intermediate of the methanol synthesis, as reported by previous researchers [19,20]. Methoxy species, which can be predicted as hydrogenation product from formate species [14,17] detected at 2824 and 2920  $\text{cm}^{-1}$ . However, the methoxy species could not be observed on the surface of undoped- $\text{TiO}_2$  photocatalyst.

Numerous reaction schemes for the photocatalytic reduction of  $\text{CO}_2$  on  $\text{TiO}_2$  based catalysts have been proposed in different studies [1,5-7]. Although the exact mechanism of methanol production from  $\text{CO}_2$  photoreduction is not absolutely clear in our present study, the results obtained in the current analysis show good correspondence with the kinetics as well as *in situ* IR experiments. The appearance of formate and methoxy intermediates on the  $\text{CuO}/\text{TiO}_2$  surface, while none on the undoped- $\text{TiO}_2$  catalyst, may indicate that the catalytic role of copper species as an active site is to provide methanol. In the hydrogenation of  $\text{CO}_2$ , Kakumoto [14] proposed that the methanol synthesis mainly occurs on  $\text{Cu}^+$  site which the linear adsorption of  $\text{CO}_2$  dominantly take place. The mechanism of methanol synthesis on the  $\text{CuO}/\text{TiO}_2$  surface is proposed, as shown in the following equations (2 - 5) followed by mechanism scheme in the Fig. 9.

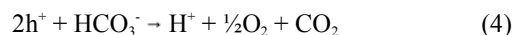
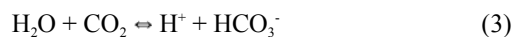
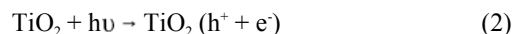


Photo-excited electrons ( $e^-$ ) and positive hole ( $h^+$ ) are generated when incident photons are absorbed in the surface of  $\text{CuO}/\text{TiO}_2$  catalyst. The holes first react with water and/or  $\text{H}_2\text{CO}_3$ , resulting in producing hydrogen ions ( $\text{H}^+$ ) and oxygen. Moreover generated electrons may be consumed via the reduction of  $\text{H}^+$  forming radicals of  $\bullet\text{H}$ . At the same time,  $\text{CO}_2$  is adsorbed on  $\text{Cu}^+$  site linearly. Furthermore, it is suggested that the sequential interaction of  $\bullet\text{H}$  radicals and  $\text{H}^+$  with the adsorbed state

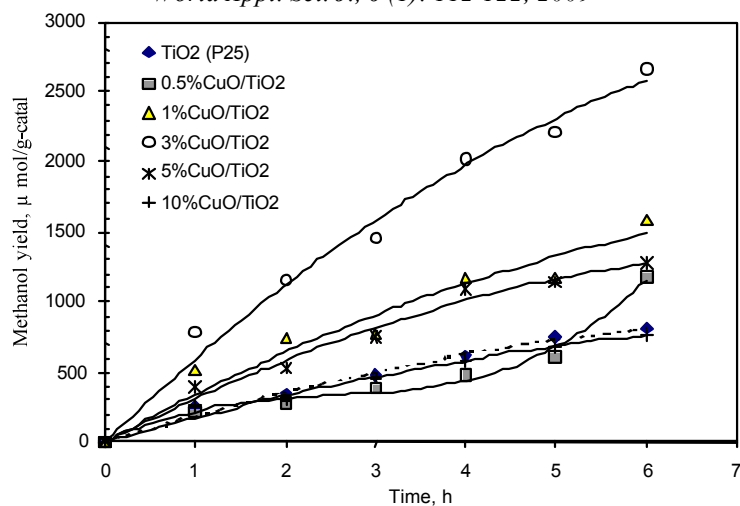


Fig. 5: Time dependence on the methanol yields of various catalysts at 333 K and UV irradiation

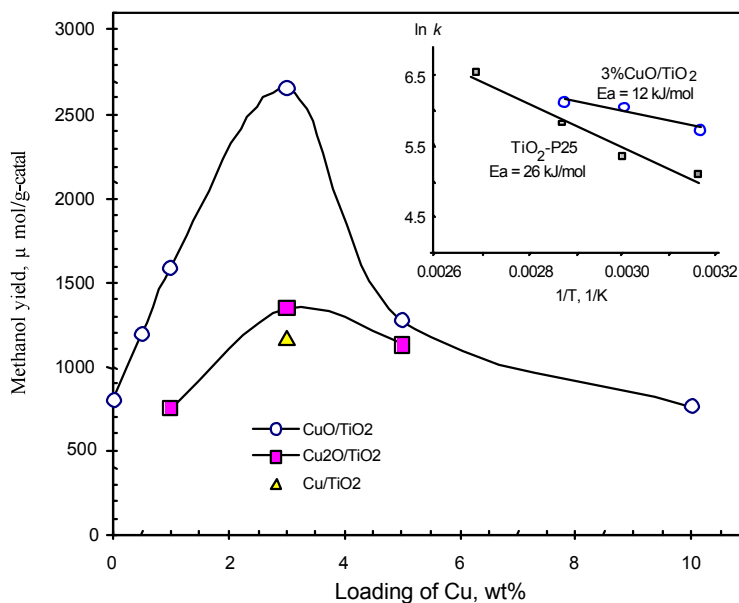


Fig. 6: Effect of copper loading amount on methanol yield under 333 K and 6 h UV irradiation. Inset: Arrhenius plot for  $\text{TiO}_2$  and 3% $\text{CuO/TiO}_2$  catalysts

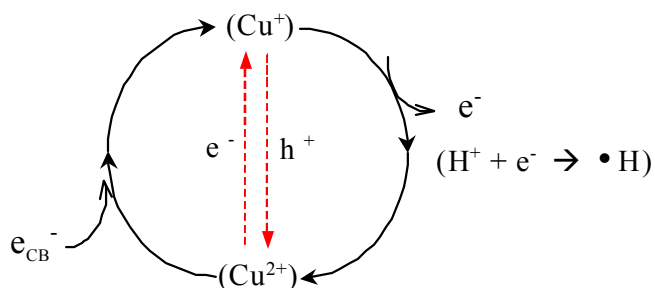


Fig. 7: Schematic of the redox cycle of  $\text{Cu}^{2+}/\text{Cu}^+$  system in the photoreduction of  $\text{CO}_2$



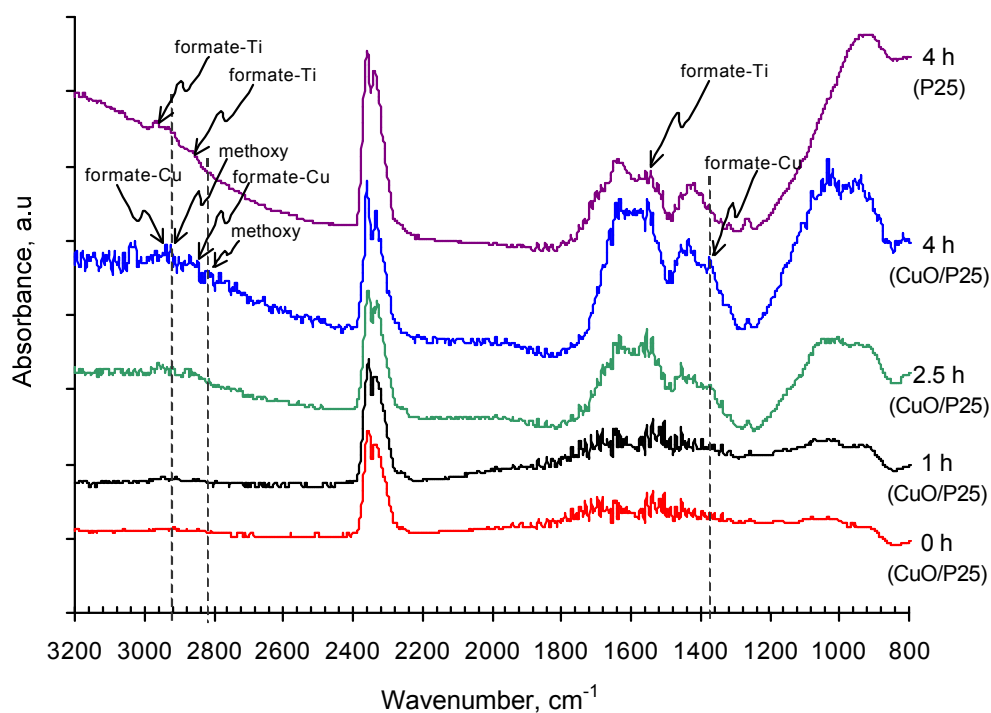


Fig. 8: *In situ* IR spectra of 3% CuO/TiO<sub>2</sub> catalyst during gas phase CO<sub>2</sub> photoreduction (Mol ratio of H<sub>2</sub>O/CO<sub>2</sub> = 5, CO<sub>2</sub> = 330 μmol, T = 333 K)

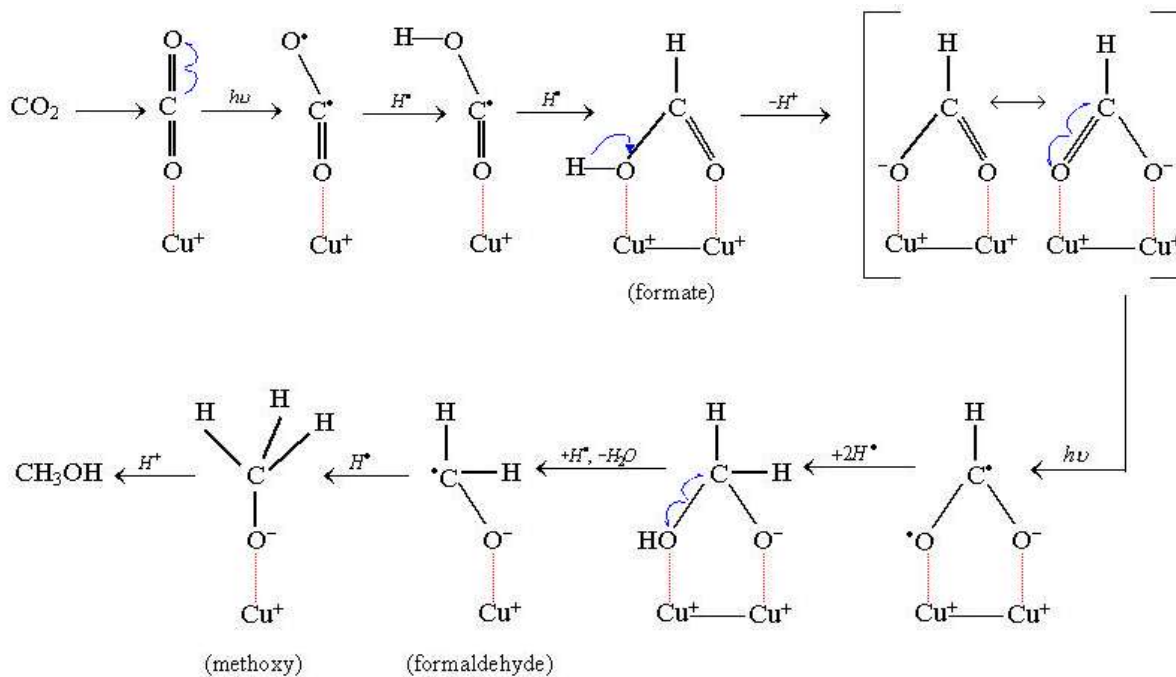


Fig. 9: Scheme of CO<sub>2</sub> photoreduction mechanism on CuO/TiO<sub>2</sub> catalyst

of CO<sub>2</sub> on Cu<sup>+</sup> surfaces lead to the formation of methanol via the formate and methoxy intermediates.

## CONCLUSIONS

The photocatalytic reduction of CO<sub>2</sub> with H<sub>2</sub>O at the liquid/solid interface of copper-doped titania photocatalysts have been performed, giving methanol as a main product. Experimental results demonstrated that the photocatalysts with a various dopant species (CuO, Cu<sub>2</sub>O, or Cu<sup>o</sup>) can be synthesized by an improved-impregnation method via the reduction-oxidation steps. The optimal Cu-loaded TiO<sub>2</sub> (in this study, 3 wt %) has shown to be a highly efficient photocatalyst for CO<sub>2</sub> photoreduction. It has been revealed that CuO is the dopant species that actually has a significant contribution in improving the CO<sub>2</sub> photoreduction over TiO<sub>2</sub> matrix. The apparent activation energy (E<sub>a</sub>) for 3%CuO/TiO<sub>2</sub>, in the working temperature (316-373 K), is lower than that for Degussa P25. This suggests that CuO dopant species plays a role as a catalytic site in enhancing the production of methanol. *in situ* FTIR experiment revealed that the methanol was also catalytically synthesized on the CuO/TiO<sub>2</sub> surface by producing formate and methoxy intermediates. Therefore, the considerable improvement of CO<sub>2</sub> reduction photoefficiency by CuO dopant is proposed due to the double effects of the dopant: i.e. as an electron trapper and a catalytic active site.

## ACKNOWLEDGMENT

The authors would like to thank the Indonesian Petroleum and Gas Corporation (PERTAMINA) for financially supporting this research under contract no. 3230/10000/97-SO.

## REFERENCES

1. Tseng, I.H., W.C. Chang and J.C.S. Wu, 2002. Photoreduction of CO<sub>2</sub> using Sol-Gel Derived Titania and Titania-Supported Copper Catalysts. *Appl. Catal. B: Environ.*, 37: 37-48.
2. Adachi, K., K. Ohta and T. Mizuno, 1994. Photocatalytic Reduction of Carbon Dioxide to Hydrocarbon using Copper-Loaded Titanium Dioxide. *Sol. Energy*, 53(2): 187-190.
3. Yamashita, H., H. Nishiguchi, N. Kamada and M. Anpo, 1994. Photocatalytic Reduction of CO<sub>2</sub> with H<sub>2</sub>O on TiO<sub>2</sub> and Cu/TiO<sub>2</sub> Catalysts. *Res. Chem. Intermed.*, 20(8): 815-823.
4. Tseng, I.H. and J.C.S. Wu, 2004. Chemical states of metal-loaded titania in the photoreduction of CO<sub>2</sub>. *Catal. Today*, 97(2-3): 113-119.
5. Tan, S.S., L. Zou and E. Hu, 2006. Photocatalytic reduction of carbon dioxide into gaseous hydrocarbon using TiO<sub>2</sub> pellets. *Catal. Today*, 115: 269-273.
6. Liu, S., Z. Zhao and Z. Wang, 2007. Photocatalytic reduction of carbon dioxide using sol-gel derived titania-supported CoPc catalysts. *Photochem. Photobiol. Sci.*, 6: 695-700.
7. Subrahmanyam, M., S. Kaneco and N. Alonso-Vante, 1999. A screening for the photo reduction of carbon dioxide supported on metal oxide catalysts for C<sub>1</sub>-C<sub>3</sub> selectivity. *Appl. Catal. B: Environ.*, 23(2-3): 169-174.
8. Nguyen, T.V. and J.C.S. Wu, 2008. Photoreduction of CO<sub>2</sub> to fuels under sunlight using optical-fiber reactor. *Sol. Energy Mater. Sol. Cells*, 92(8): 864-872.
9. Chiang, K., R. Amal and T. Tran, 2002. Photocatalytic degradation of cyanide using titanium dioxide modified with copper oxide. *Adv. Environ. Res.*, 6(4): 471-485.
10. Mizuno, T., H. Tsutsumi and K. Ohta, 1994. Photocatalytic Reduction of CO<sub>2</sub> with Dispersed TiO<sub>2</sub>/Cu Powder Mixtures in Supercritical CO<sub>2</sub>. *Chem. Lett.*, pp: 1533-1536.
11. Xu, B., L. Dong and Y. Chen, 1998. Influence of CuO loading on dispersion and reduction behavior of CuO/TiO<sub>2</sub> (anatase) system. *J. Chem. Soc., Faraday Trans.*, 94(13):1905-1909.
12. Sanchez, E. and T. Lopez, 1995. Effect of the preparation method on the band gap of titania and platinum-titania sol-gel materials. *Mater. Lett.*, 25: 271-275.
13. Anpo, M. and M. Takeuchi, 2003. The design and development of highly reactive titanium oxide photocatalysts operating under visible light irradiation. *J. Catal.*, 216: 505-516.
14. Kakumoto, T., 1995. A Theoretical Study for the CO<sub>2</sub> Hydrogenation Mechanism on Cu/ZnO Catalyst. *Energy Convers. Mgmt.*, 36(6-9): 661-664.
15. Saladin, F. and I. Alxneit, 1997. Temperature dependence of the photochemical reduction of CO<sub>2</sub> in the presence of H<sub>2</sub>O at the solid/gas interface of TiO<sub>2</sub>. *J. Chem. Soc., Faraday Trans.*, 93(23): 4159-4163.
16. Guan, G., T. Kida, T. Harada, M. Isayama and A. Yoshida, 2003. Photoreduction of carbon dioxide with water over K<sub>2</sub>Ti<sub>6</sub>O<sub>13</sub> photocatalyst combined with Cu/ZnO catalyst under concentrated sunlight. *Appl. Catal. A: General*, 249(1): 11-18.

17. Nomura, N., T. Tagawa and S. Goto, 1998. *In situ* FTIR study on hydrogenation of carbon dioxide over titania-supported copper catalysts. Appl. Catal., A: General, 166: 321-326.
18. Burcham, L.J., M. Badlani and I.E. Wachs, 2001. The Origin of the Ligand in Logam Oxide Catalysts: Novel Fixed-Bed *in situ* Infrared and Kinetic Studies during Methanol Oxidation. J. Catal., 203: 104-121.
19. Fisher, I.A. and A.T. Bell, 1997. *In situ* Infrared Study of Methanol Synthesis from  $H_2/CO_2$  over Cu/SiO<sub>2</sub> and Cu/ZrO<sub>2</sub>/SiO<sub>2</sub>. J. Catal., 172: 222-237.
20. Gao, L.Z. and C.T. Au, 2000. CO<sub>2</sub> Hydrogenation to Methanol on YBa<sub>2</sub>Cu<sub>3</sub>O<sub>7</sub> Catalyst. J. Catal., 189: 1-15.